



Ramos-Román, M.J., Jiménez-Moreno, G., Toney, J., Anderson, R.S., Garcia-Alix Daroca, A., Toney, J.L., Jiménez-Espejo, F.J. and Carrión, J.S. (2016) Centennial-scale vegetation and North Atlantic Oscillation changes during the Late Holocene in the southern Iberia. *Quaternary Science Reviews*, 143, pp. 84-95. (doi:[10.1016/j.quascirev.2016.05.007](https://doi.org/10.1016/j.quascirev.2016.05.007))

This is the author's final accepted version.

There may be differences between this version and the published version. You are advised to consult the publisher's version if you wish to cite from it.

<http://eprints.gla.ac.uk/119125/>

Deposited on: 24 June 2016

Enlighten – Research publications by members of the University of Glasgow
<http://eprints.gla.ac.uk>

Centennial-scale vegetation and North Atlantic Oscillation changes during the Late Holocene in the southern Iberia

M.J. Ramos-Román¹, G. Jiménez-Moreno¹, R.S. Anderson², A. García-Alix³, J.L. Toney³, F.J. Jiménez-Espejo⁴, J.S. Carrión⁵

¹ Departamento de Estratigrafía y Paleontología, Universidad de Granada, Granada, Spain

² School of Earth Sciences and Environmental Sustainability, Northern Arizona University, Flagstaff, AZ, USA

³ School of Geographical and Earth Sciences, University of Glasgow, UK

⁴ Department of Biogeochemistry, Japan Agency for Marine-Earth Science and Technology (JAMSTEC), Yokosuka, Japan

⁵ Departamento de Biología Vegetal, Facultad de Biología, Universidad de Murcia, Murcia, Spain

Highlights

1. We studied a late Holocene vegetation and fire record from southern Spain.
2. A long-term aridification trend is observed, interrupted by shorter-scale variability.
3. This study shows humidity changes during the last 4500 yr, related to NAO changes and solar variability.

Abstract

High-resolution pollen analysis, charcoal, non-pollen palynomorphs and magnetic susceptibility have been analyzed in the sediment record of a peat bog in Sierra Nevada in southern Iberia. The study of these proxies provided the reconstruction of vegetation,

climate, fire and human activity of the last ~4500 cal yr BP. A progressive trend towards aridification during the late Holocene is observed in this record. This trend is interrupted by millennial- and centennial-scale variability of relatively more humid and arid periods. Arid conditions are recorded between ~4000 to 3100 cal yr BP, being characterized by a decline in arboreal pollen and with a spike in magnetic susceptibility. This is followed by a relatively humid period from ~3100 to 1600 cal yr BP, coinciding partially with the Iberian-Roman Humid Period, and is indicated by the increase of *Pinus* and the decrease in xerophytic taxa. The last 1500 cal yr BP are characterized by several centennial-scale climatic oscillations. Generally arid conditions from ~ 450 to 1300 CE, depicted by a decrease in *Pinus* and an increase in *Artemisia*, comprise the Dark Ages and the Medieval Climate Anomaly. Since ~ 1300 to 1850 CE pronounced oscillations occur between relatively humid and arid conditions. Four periods depicted by relatively higher *Pinus* coinciding with the beginning and end of the Little Ice Age are interrupted by three arid events characterized by an increase in *Artemisia*. These alternating arid and humid shifts could be explained by centennial-scale changes in the North Atlantic Oscillation and solar activity.

Keywords: Holocene, Southern Iberia, Pollen analysis, Fire, North Atlantic Oscillation, Solar activity

1. Introduction

Recent studies have demonstrated a response of terrestrial vegetation, atmosphere and ocean environments to changes in solar radiation (Jiménez-Moreno et al., 2008, 2013a; Fletcher et al., 2012). Occurring at the boundary between temperate, subtropical and tropical climate regimes the Mediterranean region is a key area in our attempt to understand the interactions between these environments (Alpert et al., 2006).

Numerous global paleoclimate proxy records for the Holocene show that weak changes in solar activity triggered climatic variability not only at millennial-scales (e.g.; Bond et al., 1997), but also at centennial- and decadal-scales (e.g. Bond et al., 2001; Bard et al., 2006). In addition, one of the main mechanisms influencing present climate in the Mediterranean region is the North Atlantic Oscillation (NAO) and many studies have attempted to relate atmospheric dynamics of the NAO with environmental change in this area (e.g. Lionello and Sanna., 2005). In the last years a variety of multiproxy records have been used for the reconstruction of past NAO conditions (e.g. D' Arrigo et al., 1993; Trouet et al., 2009; Olsen et al., 2012; Baker et al., 2015). These show that positive NAO conditions triggered a decrease in precipitation in the western Mediterranean area, while wetter conditions occurred during negative NAO phases.

Holocene sediment records from lakes, peat bogs and marine environments from the western Mediterranean have been very informative in relating records of vegetation, fire activity and human impact to climate change. Several high-resolution multiproxy lake records from northern and central Iberia have documented centennial-scale paleoclimate evolution for the last millennia (e.g. Martín-Puertas 2008; Morellón et al., 2011; Currás et al., 2012; Moreno et al., 2012; Corella et al., 2013). Most of the Holocene paleoclimate reconstructions in the southern Iberian Peninsula come from lake and peat deposits at low and montane altitudes, as well as from marine cores (Carrión, 2002; Carrión et al., 2001a, 2001b, 2003, 2007, 2010; Martín-Puertas et al., 2008, 2010; Nieto-Moreno et al. 2011; Moreno et al., 2012; Jiménez-Moreno et al., 2015). Studies at higher elevations are scarcer and mostly come from lake and peat bog sedimentary deposits from the Sierra Nevada range (Anderson et al., 2011; Jiménez-Moreno and Anderson, 2012; García-Alix et al., 2012, 2013; Jiménez-Moreno et al., 2013b). These studies have provided a strong record of Holocene vegetation, fire,

human impact and climate evolution at millennial- and centennial-scales. Currently this region lacks high-resolution records of change that can capture decadal-scale variations such as the NAO.

Within the region, Sierra Nevada has been a key location for paleoecological studies, due to its high elevation records for southern Europe and its sensitive alpine wetland environments (Anderson et al., 2011). Previous records from the range showed that humans influenced these alpine environments during the late Holocene, especially in the last millennium, with increases in pasturing, cultivars and *Pinus* reforestation. However, human impact in these alpine environments is minimal compared to other sites at lower elevations in the area (Anderson et al., 2011; Jiménez-Moreno and Anderson, 2012; Jiménez-Moreno et al., 2013b). Although numerous studies have suggested that the Mediterranean vegetation evolution during the Holocene was largely due to human impact (Reille and Pons, 1992; Pons and Quézel, 1998), Jalut et al. (2009) considered climate change to be a more important determining factor. Others have suggested that we are still far from understanding the correlation between vegetation, fire, climate and human activity, because of the importance of ecological factors in shaping the timing of vegetation responses to disturbances (Carrión et al., 2007).

In this paper we present a multi-proxy high-resolution study from Borreguil de la Caldera (BdlC), a peat bog that records the last ~4500 cal yr BP of vegetation, fire, human impact, and climate history from the Sierra Nevada in southern Spain. The main focus of this study is to elucidate the relationship between vegetation and fire activity with solar cyclicity and atmospheric dynamics. High-resolution studies such as the one here from Borreguil de la Caldera, with ca. 30-yr resolution for the last 1500 yr BP and ca. 120-yr resolution between approximately 4450 to 1600 cal yr BP, allow us to detect changes in the NAO through time and its impact on the environment. In addition, we

also comment on the record of human impact in the Sierra Nevada during the late Holocene.

1.1. Sierra Nevada: climate and vegetation

Sierra Nevada is a W-E aligned mountain range located in southern Spain. The range is one of the southernmost European areas to be glaciated during the Late Pleistocene (Schulte, 2002). The postglacial melting of cirque glaciers allowed the formation of lakes and wetlands. These formed on the metamorphic bedrock located at elevations between 2600 to 3100 m asl. Some of these lakes have filled sediments and have transitioned to small peat bogs (Castillo Martín, 2009). Bedrock is Permotriassic and Palaeozoic metamorphic rocks mostly characterized by micashists (Martín Martín et al., 2010).

In the Sierra Nevada Range, the mean annual temperature at 2500 m asl is 4.5 °C, and the mean temperature during the snow free months is 10 ± 6 °C, but could occasionally reach 21 °C. Annual precipitation is 700 mm/yr, seasonally concentrated between October and April, mostly as snow (Oliva et al., 2009). Situated between a temperate humid climate to the north and at subtropical, arid climate to the south, its location proximal to the last-glacial coastal shelves and its high-altitude make this area a particular vegetation hotspot in southern Europe (Carrión et al. 2008; González-Sampériz, 2010; Anderson et al., 2011; Jiménez-Moreno and Anderson, 2012; Jiménez-Moreno et al., 2013b). Sierra Nevada is one of the most important centers of plant diversity in the western Mediterranean region. With more than 2100 vascular taxa (species and subspecies) catalogued, it accounts for nearly 30% of the entire vascular flora of the Iberian Peninsula (Blanca, 1996, 2002). Due to the altitudinal gradient of Sierra Nevada (from 900 to more than 3400 m) this mountain range is strongly influenced by thermal and precipitation gradients allowing well-characterized

vegetation belts (Valle et al., 2003). The crioromediterranean vegetation belt characterized principally by *Festuca clementei*, *Hormatophylla purpurea*, *Erigeron frigidus*, *Saxifraga nevadensis*, *Viola crassiuscula*, and *Linaria glacialis* is the highest in the area and occurs above ~2800 m. The oromediterranean belt, between ~1900 to 2800 m, bears *Pinus sylvestris*, *Pinus nigra*, *Juniperus hemisphaerica*, *Juniperus sabina*, *Juniperus communis* subsp. *nana*, *Genista versicolor*, *Cytisus oromediterraneus*, *Hormatophylla spinosa*, *Prunus prostrata*, *Deschampsia iberica* and *Astragalus sempervirens* subsp. *nevadensis* as the most representative species. The supramediterranean belt, from approximately 1400 to 1900 m of elevation principally includes *Quercus pyrenaica*, *Quercus faginea*, *Quercus rotundifolia*, *Acer opalus* subsp. *granatense*, *Fraxinus angustifolia*, *Sorbus torminalis*, *Adenocarpus decorticans*, *Helleborus foetidus*, *Daphne gnidium*, *Clematis flammula*, *Cistus laurifolius*, *Berberis hispanicus*, *Festuca scariosa* and *Artemisia glutinosa*. The mesomediterranean between ~600 and 1400 m of elevation are characterized by *Quercus rotundifolia*, *Retama sphaerocarpa*, *Paeonia coriacea*, *Juniperus oxycedrus*, *Rubia peregrina*, *Asparagus acutifolius*, *D. gnidium*, *Ulex parviflorus*, *Genista umbellata*, *Cistus albidus* and *Cistus laurifolius* (El Aallali et al., 1998; Valle et al., 2003). The human impact over this area affected the vegetation distribution especially during the last millennium. The most important examples of human disturbance in the area are the *Olea* increase for cultivation at relatively low elevations and *Pinus* reforestation (Anderson et al., 2011; Jiménez-Moreno and Anderson 2012; Jiménez-Moreno et al., 2013b).

1.2. Borreguil de la Caldera (BdlC)

This bog presently occurs above treeline, in the crioromediterranean vegetation belt (Valle, 2003). In Sierra Nevada small bogs such as this one are locally known as “Borreguiles”, which are installed on cirque basin environments with constant moisture

characterized by tundra-like vegetation with Cyperaceae as the most representative species. Other secondary species are represented by *Nardus stricta*, *Festuca iberica*, *Leontodon microcephalus*, *Luzula hispanica*, *Ranunculus demissus*, *Sagina saginoides* subsp. *nevadensis*, *Campanula herminii*, *Saxifraga stellaris* subsp. *alpigena*, *Veronica turbicola*, *Sedum anglicum* subsp. *melanantherum*, *Festuca rivularis* and some species of briophytes. Around this peat bog other plant species occur, such as *Armeria splendens*, *Agrostis nevadensis*, *Ranunculus acetosellifolius*, *Plantago nivalis* and *Lepidium stylatum* (Molero-Mesa et al., 1992). BdlC formed part of those high-elevation wetland areas; it is a small peat bog located at 37° 03' 02" N and 3° 19' 24" W in the south face of Sierra Nevada at ~2992 m elevation (Fig. 1). It is situated right below Laguna de la Caldera, another cirque-lake basin located in the upper drainage part of the Mulhacén River. The peat bog area is 0.17 ha. The surface of the drainage basin is 62 ha and includes the Mulhacén (3479 m asl), the highest peak of the Iberian Peninsula. The area is snow-free approximately between July and October.

2. Methods

Two sediment cores, BdlC-01 and BdlC-02, were recovered in September 2013 from the center of the BdlC basin. Cores were taken with a Livingstone square-rod piston corer. The length for BdlC-01 and BdlC-02 was 56 and 51 cm, respectively. BdlC-02 was taken ca. 50 cm apart from BdlC-01. BdlC-01 was the longest core and it was used for this study.

The split sediment core BdlC-01 was described in the laboratory with respect to lithology and color (Fig. 2). Magnetic susceptibility (MS), a measure of the tendency of sediment to carry a magnetic charge (Snowball and Sandgren, 2001), was measured with a Bartington MS2E meter in SI units. MS measurements were obtained directly from the core surface every 0.5 cm for the entire length of the core (Fig. 2). Five

calibrated AMS radiocarbon dates were used to constrain the core chronology. Material used for the AMS datings was peat. Radiocarbon dates were converted to calendar year before present (cal yr BP) using the IntCal13 curve (Reimer et al., 2013) with Calib 7.1 (<http://calib.qub.ac.uk/calib/>) (Table 1). The age model for BdIC-01 was built using a constant variance model following Heegaard et al. (2005). Calculations of the expected ages and their 95% confidence intervals were made using the software package R (Development Core Team, 2013) employing the functions Cagedepth.r Cagenew.r (Heegaard et al., 2005) (Fig. 2). The sedimentary accumulation rate (SAR) was calculated based on the linear interpolation between radiocarbon dates (Fig. 2).

Samples for pollen analysis (1 cm^3) were taken every 0.5 cm throughout the core (Fig. 3). Pollen extraction methods followed a modified Faegri and Iversen (1989) methodology. Processing included the addition of *Lycopodium* spores for calculation of pollen concentration. Sediment was treated with NaOH, HCl, HF and the residue was sieved at $250\text{ }\mu\text{m}$ previous to an acetolysis solution. Counting was performed using a transmitted light microscope at $400\times$ magnification to a minimum pollen count of 300 terrestrial pollen grains. Fossil pollen was identified using published keys (Beug, 1961) and modern reference collections at University of Granada (Spain). Pollen concentration is a measure of pollen density [grains per cm^3 of sample sediment (gr/cm^3); Fig. 3]. The raw counts were transformed to pollen percentages based on the terrestrial sum, not including Cyperaceae (Fig. 3). The pollen zonation was executed by cluster analysis using eight different pollen taxa- *Pinus*, *Olea*, *Artemisia*, Poaceae, Caryophyllaceae, Cichorioideae, *Quercus* total and Other Asteraceae (CONISS; Grimm, 1987). Non-pollen palynomorphs (NPP) were found in the pollen slides including fungal spores, thecamoebians, algal spores and micro-zoological remains. The NPP percentages were calculated and represented with respect to the total pollen sum (Fig. 3). Tree pollen taxa

were grouped in arboreal pollen (AP). In addition, we calculated the Cyperaceae/Poaceae ratio (C/P ratio) (Fig. 4). This ratio has previously been used as an indicator of wet and dry conditions in bog areas (e.g., Turney et al., 2004). A cyclostratigraphic analysis was performed in the BdlC-01 pollen time series. We used the REDFIT software (Schultz and Mudelsee, 2002) on the unevenly spaced pollen time series in order to identify cyclical changes in the vegetation through spectral peaks registered at different frequencies throughout the studied core.

Samples for macrocharcoal analysis (1 cm^3) were taken every 0.5 cm through the core (Fig. 3), following the methodology described in Whitlock and Anderson (2003). In order to deflocculate the sediments, the samples were soaked in a solution of ca. 10% sodium hexametaphosphate and distilled water for two to five days. Samples were washed and sieved into a set with mesh size of 125 and 250 μm . Each subsample was counted using a stereomicroscope to 10-70x magnifications.

3. Results

3.1. Chronology and sedimentary rates

The age-depth model (Fig. 2) shows that the BdlC-01 record covers the last 4500 cal yr BP. SARs between 0.008 and 0.02 cm/yr occurred from ~23 cm to the core bottom. SAR increased to ~0.03 cm/yr between ~13 cm to the core top. The highest SAR of 0.20 cm/yr occurred right above ~ 23 to 13 cm [about 550 to 350 cal yr BP].

3.2. Lithology and magnetic susceptibility

The BdlC-01 record mostly consists of peat sediments but thin layers of clay occur at about 52 to 51 cm, coinciding with a MS spike (Fig. 2). MS data show minimum values around 20 to 17 cm, corresponding to a more fibrous peat at that depth.

MS spikes again at ~12 cm but visually we could not observe any significant lithological change.

3.4. Pollen, NPP and charcoal

A total of fifty-four pollen taxa were identified but only the most representative (taxa higher than 1%) were plotted in the pollen diagram (Fig. 3). NPP and charcoal are also displayed in Figure 3. Four pollen zones (Fig. 3) were visually identified with the help of cluster analysis using the program CONISS (Grimm, 1987). Pollen preservation was good and concentration was high from ~50,000 to 3,500,000 grains/cc. Charcoal concentration varied from 0 to 8 particles/cc. Pollen zones are described below:

3.4.1. Zone BdlC- 1 [~4500 to 1740 cal yr BP/~2600 to 200 BCE (56-40 cm)]

Zone 1 is principally characterized by the abundance of herbs and grasses such as Poaceae, with an average occurrence around 37% and Cichorioideae of ca. 22%. Other herbs such as Amaranthaceae, Caryophyllaceae, Gentianaceae and Campanulaceae also occur but with lower abundances in this zone. The AP is mainly composed of *Pinus*, with average values around 11% but there are some important peaks around 20%. Although tree pollen is dominated by *Pinus* other tree taxa occur in lesser concentrations, with *Quercus* total (ca. 2%), *Olea* (< 1%) and *Betula* (ca. 1%; not plotted in the diagram due to very low percentage) as the most representative. This pollen zone is subdivided into zones subzone-1a and subzone-1b (Fig. 3). The main characteristics that differentiate subzone 1a from 1b (at ca. 3000 cal yr BP/ca. 1050 cal BC) are the decline in Poaceae from ca. 55 to 25% and the increase in *Pinus* from ca. 10 to 20%. Other Asteraceae and Caryophyllaceae also slightly increase ca. 3-7% and ca. 2-5%, respectively. Wetland plants such as Cyperaceae also occur and show a

considerable increase (from ca. 8% to 15%) between subzone 1a/1b. Charcoal particles are rare, but show a slight increase in subzone 1b (Fig. 3).

3.4.2. Zone BdlC- 2 [~1740 to 500 cal yr BP/ ~200 BCE- 1450 CE (40-21 cm)]

The decline in Poaceae to values around 15% and the decrease in *Pinus* averaging around 5% are the most important features in this zone. *Artemisia*, other Asteraceae and, most notably, Cupressaceae become more abundant in zone 2, while Caryophyllaceae also increases. Arboreal pollen decreases remarkably, with a decline in *Pinus*, however an increase in *Quercus* total (to ca. 5%) occurred. The transition between subzone 2a/b (boundary at ~760 cal yr BP/AD 1200) is remarkable, with a prominent increase in *Artemisia* and *Quercus* total, but on the other hand, a slight decline in other Asteraceae, Caryophyllaceae and Cichorioideae. Wetland pollen shows a considerable increase, with Cyperaceae (averaging ca. 30%) and Ranunculaceae (averaging ca. 15%). Fungal remains are also present; coprophilous fungi such as Sordariales and thecamoebians show their first occurrence in this zone. The number of charcoal particles declines.

3.4.3. Zone BdlC- 3 [~500 cal yr BP to 50 cal yr BP/~1450 to 1900 CE (21 to 2.5 cm depth)]

The main feature in zone 3 is the major expansion of *Artemisia*, reaching maximum values (to ca. 40%), and the decrease in *Pinus* (to ca. 2%). A noteworthy drop in Cichorioideae (to ca. 7%) and the slight increase in evergreen *Quercus*, Cupressaceae and *Castanea* also characterize this zone. The disappearance of *Betula* and the first occurrence of *Juglans*, Cerealia, *Vitis* (not plotted in the diagram due to very low percentage) and Urticaceae-Moraceae are also remarkable. The subzone 3a/b (~160 cal yr BP/~ 1790 CE) transition is marked by an increase in arboreal pollen

mostly produced by a high increase in *Olea*, reaching maximum values (ca. 40%) at around 60 cal yr BP (AD 1890). Wetland pollen remain abundant. This zone documents a prominent increase in coprophilous fungi (*Sporormiella* and Sordariales); thecamoebians are very abundant too, showing maxima. Charcoal particles show a decrease in zone 3 in relation with the zone 2. This decrease is stronger in the end of the subzone 3b.

3.4.4. Zone BdlC- 4 [1900 CE to present (2.5 to 0 cm depth)]

Zone 4 shows the expansion of tree species with respect to zone 3, especially in *Pinus* (maximum around 30%) and evergreen *Quercus* (to ca. 10%). *Olea* remains very important in the assemblage with a very slight decline in values than in the previous subzone 3b but with two punctually stronger decreases around 1900 CE and 1980 CE. With respect to herbs, *Artemisia*, other Asteraceae and Caryophyllaceae show a decrease and Cichorioideae even disappeared. However slight increases in Amaranthaceae occurred. *Castanea*, *Juglans* and Urticaceae-Moraceae pollen disappeared at the end of the zone. Maximum values of the wetland plant Cyperaceae (ca. 60%) is observed in this zone. Thecamoebians show an increase in this zone and dung fungi continue to increase, with particular incidence for *Sporormiella* and Sordariales. Charcoal occurrence is insignificant.

3.5. Spectral Analysis

Spectral analysis was performed on the *Pinus* and *Artemisia* time-series in order to identify the presence of cyclical periodicities in the BdlC-01 record (Fig. 5). Centennial-scale cycles with periodicities around ca. 750, 650, 300, 200, 170 and 140 yr (above the 80 % confidence level) were obtained.

4. Discussion

One of the main goals of this study is to analyze the relationship of vegetation changes from the BdlC bog in the Sierra Nevada with atmospheric variations in the area and the possible links with solar variability. Integration of pollen, NPP and charcoal data are important in reconstructing the paleoclimatic and palaeoenvironmental history in this climatically sensitive region. In this study we compared our record with other local and more distant paleoclimate records, NAO reconstructions, insolation and solar output for the past 4500 cal yr BP (Trouet et al., 2009; Olsen et al., 2012; Laskar et al., 2004; Bard et al. 2000; Figs. 4 and 6). This allowed us to determine regional- and global-scale paleoclimate interpretations and inferences about the origin of these cyclic climate variations. Below we show that the BdlC Sierra Nevada alpine pollen record supports the hypothesis of a coupling between solar activity, North Atlantic atmospheric activity and environmental changes in the western Mediterranean during the Holocene.

4.1. Proxy interpretation

Variations in AP have previously been used in the Sierra Nevada as a proxy for humidity changes (Jiménez-Moreno et al., 2013b; Fig. 4). *Pinus* dominates the AP pollen sum throughout much of the Holocene in the Sierra Nevada region and this is the reason we pay special attention to this pollen taxa. *Pinus nigra* and *Pinus sylvestris* occur at present in the Sierra Nevada oromediterranean vegetation belt, between 1600-2100 m asl (Carrión et al., 2002) and 1600-2200 m asl (Castro et al., 2004), respectively. Pollen sedimentation studies show that in locations where *Pinus* is present, its percentage is approximately 50-60% of the total pollen sum (Andrade et al., 1994). This is confirmed in the Sierra Nevada by an ongoing moss polster analysis carried out in an altitudinal transect (Ramos-Román, in prep.). The pollen results show that where pine forest occurs the *Pinus* percentage is around 40-70 % and in places above the treeline it is around 20-30%. In the BdlC-01 record *Pinus* percentage is between 10-

30%, which suggests that *Pinus* forest never occurred at such high-elevation in the Sierra Nevada during the late Holocene and that these pollen grains come from lower elevations (Anderson et al., 2011).

On the other hand, increases in xerophyte pollen (e.g., *Artemisia*) have been used as an indication of aridity in the Mediterranean region (Carrión et al., 2001a; 2007; 2010; Anderson et al., 2011; Jiménez-Moreno and Anderson, 2012, Jiménez-Moreno et al., 2013b). In this study we also used xerophyte pollen to elucidate climatic shifts. In addition, the widely-used Cyperaceae – Poaceae pollen ratio (C/P ratio; Cour et al., 1999; Turney et al., 2004; Mensing et al., 2007) was used as a paleoclimate proxy to record the local vegetation response to fluctuations between wetter and drier bog conditions. Alternating high pollen percentages of Cyperaceae and Poaceae suggest that the bog frequently changed between wetter (high C/P ratio) and drier (low C/P ratio) states (Jiménez-Moreno et al., 2008).

Charcoal analysis is based on the accumulation of charcoal particles in sedimentary basins during or following a fire event. Gaussian models suggest that particles smaller than 100 μm travel well beyond 100 m and only very small particles can travel long distances (Whitlock and Anderson, 2003). The charcoal particles that we quantified were $>100 \mu\text{m}$, between 250 and 125 μm , suggesting a local source of charcoal. However Anderson et al. (2011) suggest that during the Holocene in this alpine area in the Sierra Nevada, charcoal particles probably came from fires at lower elevation.

4.2. Aridification trend during the late Holocene

Our data document an increasing trend in dryness in this area during the past 4500 cal yr BP (Fig. 4) as shown by the progressive decrease in natural forest species and the increase in xerophytes such as *Artemisia*. This agrees with previous

paleoclimatic studies in the western Mediterranean, which document a progressive aridification trend since ~7000 cal yr BP (Carrión et al., 2002; Fletcher and Sánchez Goñi, 2008; Jalut et al., 2009; Carrión et al., 2010; Anderson et al., 2011; Jiménez-Moreno et al., 2012, 2015). Jiménez-Moreno et al. (2012, 2015) suggested that semi-desert expansion and Mediterranean forest decline during the late Holocene in this area could be explained by decreasing summer insolation (Laskar et al., 2004; Fig. 4). Reduced summer insolation could have produced lower sea-surface temperatures (Marchal et al., 2002), generating a decrease in the land–sea contrast that would be reflected in a reduction of the wind system and a reduced precipitation gradient from sea to shore during the fall–winter season. Also, a reorganization of the general atmospheric circulation with a northward shift of the westerlies – a long-term enhanced positive NAO trend – has been interpreted, inducing drier conditions in this area (Magny et al., 2012). Declining summer insolation at these latitudes would have negatively affected the growing season due to cooling, producing further forest decline (Fletcher et al., 2007).

An interesting feature in the BdIC-01 record is the increasing trend in wetland plants (Cyperaceae) and the decrease in grasses (Poaceae) during the late Holocene (see C/P ratio; Fig. 4). Although this contrasts with the aridification trend discussed above, we suggest that this may be explained by two local processes. First, the decrease in summer insolation could have caused wetland and aquatic plants to have greater surface runoff water availability for longer in the summer, due to greater persistence of snowbanks upstream and a meltwater more slowly, providing a better local environment for Cyperaceae. Second, the progressive sediment infilling of the basin could have created a broader bog surface profile producing a greater surface wetland environment for Cyperaceae expansion. This increase in wetland plants during the late Holocene is in

agreement with an increase in Cyperaceae pollen in the nearby record of Borreguil de la Virgen (Jiménez-Moreno and Anderson, 2012). García-Alix et al. (2012), who studied the geochemistry from this site explained this change as the transition from a lacustrine to a full bog environment [an increase in C/N ratios and a decrease in Carbon isotopes ($\delta^{13}\text{C}$)].

4.3. Millennial-scale environment and climate change

Previous paleoecological records are available from other alpine wetlands from the Sierra Nevada (Anderson et al., 2011; Jiménez-Moreno and Anderson, 2012; Jiménez-Moreno et al., 2013b). The BdIC improves on the late Holocene record of paleoenvironmental and paleoclimates through high-resolution analysis of pollen and other proxies. Our high-resolution analysis here shows that the late Holocene progressive aridification trend is climatically more complex than originally demonstrated (Fig. 4).

4.3.1. Arid interval between ~4000 and ~3100 cal yr BP

The pollen record from BdIC-01 begins with a relatively small peak in *Pinus* between 4500 and 4200 pointing to relatively humid climate but a trend to arid conditions occurred later on, starting around 4000 cal yr BP. This relatively dry period comprises part of the pollen subzone-1a and is mainly distinguished by the lowest percentage in AP, very low abundance of *Pinus* and very low occurrence of charcoal particles. The C/P ratio also shows a decreasing trend, indicating a drier bog environment. A lithological change towards clay sedimentation and a spike in MS at ~3600 cal yr BP (around 51-52 cm) is also observed at this time (Fig. 2). Drier conditions could have triggered less vegetal productivity in the bog and/or more erosion in the drainage area producing more detritic sedimentation. Our results agree with

previous studies in the area and arid conditions at this time are well documented in changes in paleoecological and geochemical proxies in the Laguna de la Mula, Sierra Nevada (Jiménez-Moreno et al., 2013b) and in several other marine records from Alboran Sea (synthesized in Martín-Puertas et al., 2010 and Fletcher et al., 2012) and terrestrial sites such as Zoñar Lake (synthesized in Martín-Puertas et al., 2010). Oliva et al. (2009) shows the occurrence of solifluction landforms between 2500 and 3000 m asl in the Sierra Nevada around 3400 cal yr BP, which they explained as cold and/or wet periods. Cold and arid conditions are inferred during this period in the western Mediterranean Sea (M3; Frigola et al., 2007) and higher Saharan dust input (Zr/Al ratio; Jiménez-Espejo et al., 2008). Aridity in the western Mediterranean area could be explained by multi-decadal persistence of positive NAO conditions at this time (Olsen et al., 2012).

4.3.2. Humid period between ~3100 and ~1600 cal yr BP

Probably the most humid period during the late Holocene in southern Iberia occurred during the well-known Iberian-Roman Humid Period (IRHP) (Martín-Puertas et al., 2009). The BdlC record shows maxima in humid conditions at this time (zone-1b) through maximum values of AP (mostly *Pinus*) previously to recent human reforestation and a decrease in xerophytic plants with a minimum in *Artemisia* (BdlC-1b pollen zone; Fig. 4). This is in agreement with other western Mediterranean paleoclimate records such as Zoñar Lake (Martín-Puertas et al., 2009), a marine core of Alboran Sea (Martín-Puertas et al., 2010) and the Laguna de la Mula in the Sierra Nevada (Jiménez-Moreno et al., 2013b). NAO reconstructions show the most negative phases during this period (Olsen et al., 2012; Baker et al., 2015; Fig. 4), which could explain high winter precipitation, the main source of moisture in this area. The smaller-scale variability observed in the pollen record, with two relative minima in AP during

this generally-humid period, could also be due to oscillations in the NAO, observed in the Olsen et al. (2012) reconstruction, further supporting the link between vegetation changes and the NAO cyclical phases. This variability is shown in AP and C/P ratios from BdlC. A first gradual transition phase from an arid period between ca. 3100 and 2800 cal yr BP is observed in the increase in AP and C/P ratio. The most humid period is observed between ca. 2800 to 2400 cal yr BP, with the maximum in AP and a high increase in C/P ratio. A relative arid period is interpreted between ca. 2400 to 1900 cal yr BP by a general decrease in AP (even though there is a peak in AP at approximately 2200 cal yr BP) and C/P ratio. A relative humid interval occurred between ca. 1900 and 1600 cal yr BP, depicted by the increase in AP and C/P ratios. Other studies in southern Iberia show variability in humidity during the IRHP. The most humid period from 2500 to 2140 cal yr BP, an arid period between 2140 to 1800 cal yr BP and a relative humid period from 1800 to 1600 cal yr BP are also observed in the record from Zoñar Lake (Martín-Puertas et al., 2009) and a very similar variability is showed in the record of Somolinos Lake (Currás et al., 2012).

The maximum macrocharcoal concentration registered in BdlC-01 coincided in time with the wettest period in the record (Figs. 3 and 4). The comparison with another records from the Sierra Nevada (Anderson et al., 2011; Jiménez-Moreno et al., 2013b) and other studies in close mountain ranges and marine records in the western Mediterranean region (Sierra de Gador [Carrión et al., 2003], Sierra de Baza [Carrión et al., 2007], Alborán Sea [Daniau et al., 2007] and Djamila, northern Morocco [Linstädter and Zielhofer, 2010]) also show an increase in fire activity during this period. This suggests that higher fire activity at this time could have been related to the presence of abundant fuel load (Daniau et al., 2007; Linstädter and Zielhofer, 2010; Jiménez-Moreno et al., 2013b). Nevertheless, two different records in Sierra de Cazorla show a

reverse trend in fire activity during this period (Carrión et al., 2001b; Carrión et al., 2002), which may be due to different characteristics in fire regimes related with precipitation (Linstädter and Zielhofer, 2010; Jiménez-Moreno et al., 2013b). For example, in typically arid and semiarid environments in the Mediterranean area fuel load limits fire regimes. However, in the less arid Mediterranean environments with a mean annual precipitation above 500-700 mm the factor for fire recurrence could have been moisture. We suggest that this could explain the different fire recurrences during this period in one of the Sierra de Cazorla records (Siles lake; Carrión et al., 2002) with an annual precipitation average of 800-1000 mm. However in the other record from the Sierra de Cazorla (Villaverde lake; Carrión et al., 2001b) a lesser annual precipitation average of around 225 mm is recorded and it is not possible to apply this hypothesis but another of the many factors controlling fire in the area. Gil-Romera et al. (2010) summarized pollen and charcoal records from southeastern Spain and showed that differences in fire regimes could be explained by variations in climate, vegetation, altitude and human activity.

4.3.3. Most Recent 1500 cal yr BP: Dark Ages, Medieval Climate Anomaly and Little Ice Age

The most recent 1500 years in the BdIC record are characterized by several centennial-scale environmental and climatic oscillations (Fig. 6). First, a generally arid period (coinciding with the majority of zone-2) occurred between ca. 1500 to 660 cal yr BP (ca. 450 to 1300 CE), depicted by a progressive decrease in *Pinus* (and AP in general) and an increase in *Artemisia*. This period comprises the Dark Ages (DA) and the Medieval Climate Anomaly (MCA), between 500 to 900 CE and 900 to 1300 CE, respectively (Moreno et al., 2012). Previous studies show overall arid conditions and persistently positive NAO (low winter precipitation) during this time, supporting our

results. For example, tree-ring and speleothem analyses from Morocco and Scotland (Trouet et al., 2009; Wassenburg et al., 2013; Baker et al., 2015) and a multiproxy geochemical record from a small lake in Greenland (Olsen et al., 2012) all show a strong correlation among different paleoclimate proxies with positive NAO during that time. This also agrees with more regional marine and terrestrial studies from the Iberian Peninsula. Vegetation evolution through the MCA in central and eastern Iberia shows a general decrease in AP, principally in mesophytic taxa, and an increase in more xerophytic and heliophytic vegetation (Moreno et al., 2008; 2012; Morellón et al., 2011; Rull et al., 2011; Corella et al., 2013) also suggesting aridity. Further, Moreno et al. (2012) reviewed paleoclimate proxies for the MCA from the Iberian Peninsula and showed a general decline in lake levels in northeast and southeast Iberia (Martín-Puertas et al., 2010; Morellón et al., 2011) with major Saharan eolian input in the westernmost part of the Mediterranean Sea (Nieto-Moreno et al., 2011).

The last ca. 700 cal yr BP (between 1300 CE and present) are characterized by rapid and pronounced centennial-scale oscillations (Fig. 6). Four periods depicted by relatively higher *Pinus* (and AP) and centered at ca. 1300, 1410, 1550-1620 and 1810 CE occurred, most likely indicating enhanced humid conditions. The first and last of these humid periods coincided with the beginning and end of the Little Ice Age (LIA; from ca. 1300 to 1850 CE). It is worth noting that charcoal peaks occurred immediately after these humid periods, supporting the hypothesis of the availability of fuel conditioning fire activity discussed above (Figs. 3 and 4). Continuing with our reasoning above, wetter climatic conditions during the LIA period are probably related to negative NAO conditions, which produces a general increase in winter precipitation in the area (Trouet et al., 2009; Fig. 6). These alternate with three arid events are also observed during the LIA, perhaps related to cyclical changes in NAO states as

previously observed in Trouet et al. (2009) (Fig. 6). The strong visual covariation between these humid-to-arid events, NAO states and solar activity (sunspots) observed in the last few centuries (Bard et al., 2000) could indicate a strong coupling between changes in solar activity, atmospheric variations and vegetation changes here. Low solar activity during the Wolf, Spörer, Maunder and Dalton minima could have triggered persistent negative NAO conditions, enhancing winter precipitation in the area that would produce increases in forest species (i.e., *Pinus*) and decreases in *Artemisia* (Fig. 6). Morellón et al. (2011) also observed increases in *Pinus nigra* and *P. sylvestris* as well as higher lake levels in a montane lake in the Pre-Pyrenees (northeastern Spain) coinciding in time with minima in solar activity. The increase in *Pinus* during the last century (zone-4) is more difficult to interpret due to the major influence of human activity in the area that could have modified the landscape (see section below).

4.4. Centennial-scale vegetation, solar and atmospheric changes

Previous Holocene studies suggest that small variations in solar activity could have produced changes in the atmospheric dynamics at millennial-, centennial- and decadal-scales (e.g., Bard et al., 2000; Bond et al., 2001; Hu et al., 2003; Martín-Puertas et al., 2012). Times series analysis on the BdlC-01 record reveals centennial-scale periodicities around ca. 750, 650, 300, 200, 170, 140 and 120 years above the 80% confidence level (Fig. 5). Some of these periodicities are very similar to well-known atmospheric variations (e.g. NAO) and solar cycles, suggesting a link between changes in the vegetation and thus climate in this area, mostly conditioned by NAO modes, with solar activity. The 650-yr cycle could be in relation with the 650-yr cycle shown in a record from the East Alboran Sea basin (Rodrigo-Gámiz et al., 2014) related with North Atlantic thermohaline circulation and sea surface temperatures. With respect to the 300-yr cycle, Bond et al. (2001) found a similar cycle of ca. 300 yr in the ice rafting debris

record, this cycle is also shown in the NAO reconstruction (Olsen et al., 2012). The 200-yr period could be linked with the 208-yr Suess cycle (Damon and Sonnett, 1991). The 170-yr cycle shows similar periodicities with the NAO reconstruction (Olsen et al., 2012). Other pollen records also point to a relationship between vegetation changes and the solar-climate activity and some similar centennial-scale cycles at 197, 212, 222, 292 and 750 yr are shown in an alpine bog record from New Mexico (Jiménez-Moreno et al., 2008), coinciding with the BdlC-01 record at ca. 200, 300 and 750 yr periodicities. Therefore, these studies show similar millennial- and centennial-scale changes in vegetation related with solar and North Atlantic atmospheric oscillations that could be of hemispheric-scale.

4.5. Human impact

Evidences of human impact in the BdlC record began to appear prior to the Industrial Era, notably since ca. 1500 CE (zones BdlC-3 and BdlC-4). Coprophilous fungi such as Sordariales are first recovered from sediments beginning about 1500 years ago, but strongly increase in abundance and frequency in the last ~400 years contemporaneous with the appearance of *Sporormiella* (Fig. 7). This trend correlates with other locations in Sierra Nevada, specifically with the BdlV and LdRS records, where *Sporormiella* consistently occurs during the last 500 yr (Jiménez-Moreno and Anderson, 2012) and 1000 yr (Anderson et al., 2011), respectively. This increase is probably due to the introduction of livestock and grazing at high elevation in the Sierra Nevada (Anderson et al., 2011; Jiménez-Moreno and Anderson, 2012). Nearly contemporaneously, an increase in thecamoebians occurred in the BdlC record (Fig. 7). A similar occurrence in the BdlV record over the last 150 cal yr BP was interpreted by Jiménez-Moreno and Anderson (2012) as being due to a nutrient enrichment of the wetland by livestock that frequented the bogs.

The most recent centuries witnessed an increase in AP, principally from *Pinus* and *Olea* pollen (Figs. 4 and 7) in the BdIC-01 record. Anderson et al. (2011) suggested the increase in *Olea* paralleled an increase in olive oil production in the last century. The same pattern identified in the BdIV (Jiménez-Moreno et al., 2012) and LdlM (Jiménez-Moreno et al., 2013b) records shows this is a regional event. The increase in *Pinus* is associated with *Pinus sylvestris* plantation (Anderson et al., 2011). This reforestation commenced in the middle of the 20th century to reverse human deforestation in the preceding centuries (Valbuena-Carabaña et al., 2010).

5. Conclusions

The details recorded in the BdIC cores help to clarify the potential relationship between environmental changes in the western Mediterranean, atmospheric dynamics of the NAO and solar activity variations during the late Holocene. The overall climatic reconstructions using pollen, charcoal and NPP from the BdIC-01 record confirms previous evidence of an increasingly arid trend in climate during the late Holocene. However, our high-resolution multi-proxy analysis of the BdIC record provides a greater understanding of centennial- to decadal-scale climate change, recording rapid oscillation between relatively arid and humid intervals in this area during key-periods of the late Holocene such as the IRHP, MCA and LIA. This strong relationship is further supported in this record by correlation of these centennial-scale humidity shifts at very similar times, and with amplitudes and periodicities coinciding with previously published Mediterranean regional records, NAO reconstructions and with evidence of solar activity variations. This study has then allowed us to associate persistently positive NAO conditions with drier periods and negative NAO conditions with wetter climate in the Mediterranean region. Further, our study documents that fire activity during the late Holocene in our region is probably connected with vegetation fuel load, also in

agreement with other studies in the western Mediterranean, demonstrating that climate is a crucial factor in fire dynamics. Although anthropogenic impact is evident in the last centuries in the Sierra Nevada, our work demonstrates that, overall, climate is the most important trigger for vegetation change.

Acknowledgements

The support for the present study derives from the project P11-RNM 7332 funded by Consejería de Economía, Innovación, Ciencia y Empleo de la Junta de Andalucía, the project CGL2013-47038-R funded by Ministerio de Economía y Competitividad of Spain and Fondo Europeo de Desarrollo Regional FEDER and the research group RNM0190 (Junta de Andalucía). M.J.R.-R. acknowledges the PhD funding provided by Consejería de Economía, Innovación, Ciencia y Empleo de la Junta de Andalucía (P11-RNM 7332). Charcoal analysis was completed while M.J.R.-R. was a resident scholar at Northern Arizona. A.G.-A. was supported by a Marie Curie Intra-European Fellowship of the 7th Framework Programme for Research, Technological Development and Demonstration (European Commission). We would also like to thank two anonymous reviewers and the editor (Neil Roberts) for their valuable suggestions.

References

- Alpert, P., Baldi, M., Ilani, R., Krichak, S., Price, C., Rodó, X., Saaroni, H., Ziv, B., Kishcha, P., Barkan, J., Mariotti, A., Xoplaki, E., 2006. Relations between Climate Variability in Mediterranean region and the Tropics: ENSO, South Asian and African Monsoons, Hurricanes and Sahara Dust. In: Lionello, P., Malanotte-Rizzoli, P., Boscolo, R. (Eds.), *Mediterranean Climate Variability, Developments in earth and Environmental Sciences*, 4. Elsevier, Amsterdam, pp. 149–172.
- Anderson, R.S., Jiménez-Moreno, G., Carrión, J.S., Pérez-Martínez, C., 2011. Holocene

vegetation history from Laguna de Río Seco, Sierra Nevada, southern Spain. *Quaternary Science Reviews* 30, 1615–1629.

Andrade, A., Valdeolmillos, A., Ruíz-Zapata, B., 1994. Modern pollen spectra and contemporary vegetation in the Paramera Mountain range (Ávila, Spain). *Review of Palaeobotany and Palynology* 82, 127-139.

Baker, A., Hellstrom, J.C., Kelly, B. F. J., Mariethoz, G., Trouet, V., 2015. A composite annual-resolution stalagmite record of North Atlantic climate over the last three millennia. *Scientific Reports*, 5,1-8.

Bard, E., Raisbeck, G., Yiou, F., Jouzel, J., 2000. Solar irradiance during the last 1200 years based on cosmogenic nuclides. *Tellus B*, 52(3), 985-992.

Bard E., Frank M., 2006. Climate change and solar variability: What's new under the sun? *Earth and Planetary Science Letters* 248, 1–14.

Blanca, G., 1996. Diversidad y protección de la flora vascular de Sierra Nevada (Granada, España). In: Chacón Montero, J., Rosúa Campos, J.L. (Eds.), *Sierra Nevada. Conservación y Desarrollo Sostenible*, vol. 2, pp. 245-269. Madrid.

Blanca G., López, M.R., Lorite, J., Martínez, M.J., Molero, J., Quintas, S., Ruíz, M., Varo, M.A., Vidal, S., 2002. *Flora amenazada y endémica de Sierra Nevada*. Universidad de Granada. Consejería de Medio Ambiente de la Junta de Andalucía, Granada, 410 p.

Beug, H.-J., 1961. *Leitfaden der Pollenbestimmung für Mitteleuropa und angrenzende Gebiete*. Fischer, Stuttgart, 65pp.

Bond, G., Showers, W., Cheseby, M., Lotti, R., Almasi, P., Priore, P., Cullen, H., Hajdas, I., Bonani, G., 1997. A pervasive millennial-scale cycle in North Atlantic Holocene and glacial climates. *Science* 278, 1257-1266.

Bond, G., Kromer, B., Beer, J., Muscheler, R., Evans, M.N., Showers, W., Hoffmann, S., Lotti-Bond, R., Hajdas, I., Bonani, G., 2001. Persistent solar influence on North Atlantic climate during the Holocene. *Science* 278, 1257–1266.

Carrión, J.S., 2002. Patterns and processes of Late Quaternary environmental change in a montane region of southwestern Europe. *Quaternary Science Reviews* 21, 2047-2066.

Carrión, J.S., Munuera, M., Dupré, M., Andrade, A., 2001a. Abrupt vegetation changes in the Segura mountains of southern Spain throughout the Holocene. *Journal of Ecology* 89, 783-797.

Carrión, J.S., Andrade, A., Bennett, K.D., Munuera, M., Navarro, C., 2001b. Crossing forest thresholds. Inertia and collapse in a Holocene sequence from south-central Spain. *The Holocene*, 11, 635–653.

Carrión, J.S., Sánchez-Gómez, P., Mota, J.F., Yll, E.I., Chaín, C., 2003. Fire and grazing are contingent on the Holocene vegetation dynamics of Sierra de Gádor, southern Spain. *The Holocene* 13, 839-849.

Carrión, J.S., Fuentes, N., González-Sampériz, P., Sánchez Quirante, L., Finlayson, J.C., Fernández, S., Andrade, A., 2007. Holocene environmental change in a montane region of southern Europe with a long history of human settlement. *Quaternary Science Reviews* 26, 1455-1475.

Carrión, J.S., Finlayson, G., Fernández, S., Allué, E., López-Sáez, A., López-García, P., Fuentes, N., Gil, G., González-Sampériz, P., 2008. A coastal reservoir of biodiversity for Upper Pleistocene human populations. *Quaternary Science Reviews* 27, 2118-2135.

Carrión, J.S., Fernández, S., Jiménez-Moreno, G., Fauquette, S., Gil-Romera, G., González-Sampériz, P., Finlayson, C., 2010. The historical origins of aridity and vegetation degradation in southeastern Spain. *Journal of Arid Environments* 74, 731-736.

- Castillo Martín, A., 2009. Lagunas de Sierra Nevada. Editorial Universidad de Granada, Granada.
- Castro, J., Zamora, R., Hódar, J.A., Gómez J.M., 2004. Seedling establishment of a boreal tree species (*Pinus sylvestris*) at its southernmost distribution limit: consequences of being in a marginal Mediterranean habitat. *Journal of Ecology*, 92, 266-277.
- Corella, J.P., Stefanova, V., El Anjoumi, A., Rico, E., Giralt, S., Moreno, A., Plata-Montero, A., Valero-Garcés, B.L., 2013. A 2500-year multi-proxy reconstruction of climate change and human activities in northern Spain: The Lake Arreo record. *Palaeogeography, Palaeoclimatology, Palaeoecology* 386, 555–568.
- Cour, P., Zheng, Z., Duzer, D., Calleja, M., Yao, Z., 1999. Vegetational and climatic significance of modern pollen rain in northwestern Tibet. *Review of Palaeobotany and Palynology* 104, 183-204.
- Currás, A., Zamora, L., Reed, J. M., García-Soto, E., Ferrero, S., Armengol, X., Mezquita-Joanes, F., Marqués, M.A., Riera, S., Julià, R., 2012. Climate change and human impact in central Spain during Roman times: High-resolution multi-proxy analysis of a tufa lake record (Somolinos, 1280m asl). *Catena*, 89 (1), 31-53.
- Damon, P.E., Sonnett, C.P., 1991. Solar and terrestrial components of the atmospheric ¹⁴C variation spectrum. In: Sonett, C.P., Giampapa, M.S., Matthews, M.S. (Eds.), *The Sun in Time*. University of Arizona Press, Tucson, AZ, USA.
- Daniau, A.L., Sánchez-Goñi, M.F., Beaufort, L., Lagoun-Défarage, F., Loutre, M.F., Duprat, J., 2007. Dansgaard–Oeschger climatic variability revealed by fire emissions in southwestern Iberia. *Quaternary Science Reviews* 26, 1369–1383.
- D'Arrigo, R. D., Cook, E.R., Jacoby, G.C., Briffa, K.R., 1993. NAO and sea surface temperature signatures in tree-ring records from the North Atlantic sector. *Quaternary Science Reviews* 12, 431–440.

R Development Core Team, 2013. R: A Language and Environment for Statistical Computing. available at: <http://www.R-project.org> ((last access: April 2013), R package version 2.13.0, 2011).

El Aallali, A., López Nieto, J.M., Pérez Raya, F., Molero Mesa, J., 1998. Estudio de la vegetación forestal en la vertiente sur de Sierra Nevada (Alpujarra Alta granadina). *Ininera Geobotanica* 11, 387–402.

Faegri, K., Iversen, J., 1989. *Textbook of Pollen Analysis*. Wiley, New York.

Fletcher, W., Boski, T., Moura, D., 2007. Palynological evidence for environmental and climatic change in the lower Guadiana valley (Portugal) during the last 13,000 years. *The Holocene* 17, 479–492.

Fletcher, W.J., Sánchez Goñi, M.F., 2008. Orbital- and sub-orbital-scale climate impacts on vegetation of the western Mediterranean basin over the last 48,000 yr. *Quaternary Research* 70, 451–464.

Fletcher, W.J., Debret, M., and Sánchez Goñi, M.F., 2012: Mid-Holocene emergence of a low-frequency millennial oscillation in western Mediterranean climate: implications for past dynamics of the North Atlantic atmospheric westerlies. *The Holocene*, 23, 153-166.

Frigola, J., Moreno, A., Cacho, I., Canals, M., Sierro, F.J., Flores, J.A., Grimalt, J.O., Hodell, D.A., Curtis, J.H., 2007. Holocene climate variability in the western Mediterranean region from a deepwater sediment record. *Paleoceanography* 22 (2). doi:10.1029/2006PA001307.

García-Alix, A., Jiménez-Moreno, G., Anderson, R.S., Jiménez-Espejo, F., Delgado-Huertas, A., 2012. Holocene paleoenvironmental evolution of a high-elevation wetland in Sierra Nevada, southern Spain, deduced from an isotopic record. *Journal of Paleolimnology* 48, 471–484.

García-Alix, A., Jimenez-Espejo, F.J., Lozano, J.A., Jiménez-Moreno, G., Martínez-Ruiz, F., García Sanjuán, L., Aranda Jiménez, G., García Alfonso, E., Ruiz-Puertas, G., Anderson, R.S., 2013. Anthropogenic impact and lead pollution throughout the Holocene in Southern Iberia. *Science of the Total Environment* 449, 451-460.

Gil-Romera, G., Carrión, J.S., Pausas, J.G., Sevilla-Callejo, M., Lamb, H.F., Fernández, S., Burjachs, F., 2010. Holocene fire activity and vegetation response in South- Eastern Iberia. *Quaternary Science Reviews* 29, 1082–1092.

González-Sampériz, P., Leroy, S., Carrión, J.S., García-Antón, M., Gil-García, M.J., Figueiral, I., 2010. Steppes, savannahs and botanic gardens during the Pleistocene. *Review of Palaeobotany and Palynology* 162, 427-457.

Grimm, E.C., 1987. CONISS: a Fortran 77 program for stratigraphically constrained cluster analysis by the method of incremental sum of squares. *Computers and Geosciences* 13, 13–35.

Heegaard, E., Birks, H.J.B., Telford, R.J., 2005. Relationships between calibrated ages and depth in stratigraphical sequences: an estimation procedure by mixed-effect regression. *The Holocene* 15, 612-618.

Hu, F.S., Kaufman, D., Yoneji, S., Nelson, D., Shemesh, A., Huang, Y., Tian, J., Bond, G., Clegg, B., Brown, T., 2003. Cyclic variation and solar forcing of Holocene climate in the Alaskan subarctic. *Science* 301, 1890–1893.

Jalut, G., Dedoubat, J.J., Fontugne, M., Otto, T., 2009. Holocene circum-Mediterranean vegetation changes: climate forcing and human impact. *Quaternary International* 200, 4–18.

Jimenez-Espejo, F.J., Martínez-Ruiz, F., Rogerson, M., González-Donoso, J.M., Romero, O., Linares, D., Sakamoto, T., Gallego-Torres, D., Rueda Ruiz, J.L., Ortega-Huertas, M., Perez Claros, J.A., 2008. Detrital input, productivity fluctuations, and

water mass circulation in the westernmost Mediterranean Sea since the Last Glacial Maximum. *Geochemistry, Geophysics, Geosystems*, 9 (11). doi:10.1029/2008GC002096.

Jiménez-Moreno, G., Fawcett, P.J., Anderson, R.S., 2008. Millennial- and centennial-scale vegetation and climate changes during the late Pleistocene and Holocene from northern New Mexico (USA). *Quaternary Science Reviews*, 27, 1442-1452.

Jiménez-Moreno, G., Anderson, R.S., 2012. Holocene vegetation and climate change recorded in alpine bog sediments from the Borreguiles de la Virgen, Sierra Nevada, southern Spain. *Quaternary Research* 77, 44–53.

Jiménez-Moreno, G., Burjachs, F., Expósito, I., Oms, O., Carrancho, A., Villalaín, J.J., Agustí, J., Campeny, G., Gómez de Soler, B., Van der Made, J., 2013a. Late Pliocene vegetation and orbital-scale climate changes from the western Mediterranean area. *Global and Planetary Change*, 108, 15-28.

Jiménez-Moreno, G., García-Alix, A., Hernández-Corbalán, M.D., Anderson, R.S., Delgado-Huertas, A., 2013b. Vegetation, fire, climate and human disturbance history in the southwestern Mediterranean area during the late Holocene. *Quaternary Research* 79: 110–122.

Jiménez-Moreno, G., Rodríguez-Ramírez, A., Pérez-Asensio, J.N., Carrión, J.S., López-Sáez, J.A., Villarías-Robles, J.J.R., Celestino-Pérez, S., Cerrillo-Cuenca, E., Ángel León, A., Contreras, C., 2015. Impact of late-Holocene aridification trend, climate variability and geodynamic control on the environment from a coastal area in SW Spain. *The Holocene*, 25, 607-617.

Laskar, J., Robutel, P., Joutel, F., Gastineau, M., Correia, A.C.M., Levrard, B., 2004. A long term numerical solution for the insolation quantities of the Earth. *Astronomy and Astrophysics* 428, 261–285.

Linstädter, A., Zielhofer, C., 2010. Regional fire history shows abrupt responses of Mediterranean ecosystems to centennial-scale climate change (*Olea–Pistacia* woodlands), NE Morocco. *Journal of Arid Environments* 74, 101–110.

Lionello, P., Sanna, A., 2005. Mediterranean wave climate variability and its links with NAO and Indian Monsoon. *Climate Dynamic* 25, 611–623.

Magny, M., Peyron, O., Sadori, L., Ortu, E., Zanchetta, G., Vannièrè, B., Tinner, W.S., 2012. Contrasting patterns of precipitation seasonality during the Holocene in the south- and north-central Mediterranean. *Journal of Quaternary Science*, 27, 290–296.

Marchal, O., Cacho, I., Stocker, T.F., Grimalt, J.O., Calvo, E., Martrat, B., Shackleton, N., Vautravers, M., Cortijo, E., van Kreveld, S., Andersson, C., Koç, N., Chapman, M., Sbaffi, L., Duplessy, J.-C., Sarnthein, M., Turon, J.-L., Duprat, J., Jansen, E., 2002. Apparent long-term cooling of the sea surface in the northeast Atlantic and Mediterranean during the Holocene. *Quaternary Science Reviews* 21, 455–483.

Martín Martín, J.M., Braga Alarcón, J.C., Gómez Pugnairè, M.T., 2010. Geological Routes of Sierra Nevada. Regional Ministry for the Environment, Junta de Andalucía.

Martín-Puertas, C., Valero-Garcés, B.L., Mata, P., González-Sampèriz, P., Bao, R., Moreno, A., Stefanova, V., 2008. Arid and humid phases in southern Spain during the last 4000 years: the Zoñar Lake record, Córdoba. *The Holocene* 40, 195–215.

Martín-Puertas, C., Valero-Garcés, B.L., Brauer, A., Mata, M.P., Delgado-Huertas, A., Dulsky, P., 2009. The Iberian-Roman Humid Period (2.6–1.6 cal yr. BP) in the Zoñar Lake varve record (Andalucía, southern Spain). *Quaternary Research* 71, 108–120.

Martín-Puertas, C., Jiménez-Espejo, F., Martínez-Ruiz, F., Nieto-Moreno, V., Rodrigo, M., Mata, M.P., Valero-Garcés, B.L., 2010. Late Holocene climate variability in the southwestern Mediterranean region: an integrated marine and terrestrial geochemical approach. *Climate of the Past* 6, 807–816.

- Martín-Puertas, C., Matthes, K., Brauer, A., Muscheler, R., Hansen, F., Petrick, C., Aldahan, A., Possnert, G., van Geel, B., 2012. Regional atmospheric circulation shifts induced by a grand solar minimum. *Nature Geoscience*, 5(6), 397-401.
- Mensing, S.A., Smith, J., Allan, M., Norman, K.B., 2007. Extended drought in the Great Basin western North America in the last two millennia reconstructed from pollen records. *Quaternary International* 188, 79-89.
- Molero Mesa, J., Pérez Raya, F., Valle Tendero, F., 1992. Parque Natural de Sierra Nevada. Ed. Rueda, Madrid.
- Morellón, M., Valero-Garcés, B., González-Sampériz, P., Vegas-Vilarrúbia, T., Rubio, E., Rieradevall, M., Delgado-Huertas, A., Mata, P., Romero, Ó., Engstrom, D.R., López-Vicente, M., Navas, A., Soto, J., 2011. Climate and human signatures during the medieval warm period and the little ice age in the Spanish pre-Pyrenees: the Lake Estanya record. *Journal of Paleolimnology* 46(3), 423-452.
- Moreno, A., Valero-Garcés, B.L., González-Sampériz, P., Rico, M., 2008. Flood response to rainfall variability during the last 2000 years inferred from the Taravilla Lake record (Central Iberian Range, Spain). *Journal of Paleolimnology* 40, 943-961.
- Moreno, A., Pérez, A., Frigola, J., Nieto-Moreno, V., Rodrigo-Gámiz, M., Martrat, B., González-Sampériz, P., Morellón, M., Martín-Puertas, C., Corella, J.P., Belmonte, Á., Sancho, C., Cacho, I., Herrera, G., Canals, M., Grimalt, J.O., Jiménez- Espejo, F., Martínez-Ruiz, F., Vegas-Vilarrúbia, T., Valero-Garcés, B.L., 2012. The Medieval Climate Anomaly in the Iberian Peninsula reconstructed from marine and lake records. *Quaternary Science Reviews* 42, 16–32.
- Nieto-Moreno, V., Martínez-Ruiz, F., Giral, S., Jiménez-Espejo, F., Gallego-Torres, D., Rodrigo-Gámiz, M., García-Orellana, J., Ortega-Huertas, M., de Lange, G.J., 2011.

Tracking climate variability in the Western Mediterranean during the Late Holocene: a multiproxy approach. *Climate of the Past* 7, 1395-1414.

Oliva, M., Schulte, L. and Gómez Ortiz, A., 2009. Morphometry and Late Holocene activity of solifluction landforms in the Sierra Nevada (Southern Spain). *Permafrost and Periglacial Processes* 20(4): 369–382.

Olsen, J., Anderson, N. J., Knudsen, M. F., 2012. Variability of the North Atlantic Oscillation over the past 5,200 years. *Nature Geoscience*, 5, 808-812.

Pons, A., Quézel, P., 1998. A propos de la mise en place du climat méditerranéen. *Comptes Rendus de l'Académie des Sciences-Series IIA-Earth and Planetary Science*, 327(11), 755-760.

Reille M., Pons A., 1992. The ecological significance of sclerophyllous oak forests in the western part of the Mediterranean basin: a note on pollenanalytical data. *Vegetatio* 99-100, 13-17.

Reimer, P.J., Bard, E., Bayliss, A., Beck, J.W., Blackwell, P.G., Bronk Ramsey, C., Buck, C.E., Cheng, H., Edwards, R.L., Friedrich, M., Grootes, P.M., Guilderson, T.P., Hafflidason, H., Hajdas, I., Hatté, C., Heaton, T.J., Hoffmann, D.L., Hogg, A.G., Hughen, K.A., Kaiser, K.F., Kromer, B., Manning, S.W., Niu, M., Reimer, R.W., Richards, D.A., Scott, M., Southon, J.R., Staff, R.A., Turney, C.S.M., van der Plicht, J., 2013. IntCal13 and Marine13 radiocarbon age calibration curves 0–50,000 years cal BP. *Radiocarbon* 55, 1869-1887.

Rodrigo-Gámiz, M., Martínez-Ruiz, F., Rodríguez-Tovar, F.J., Jiménez-Espejo, F.J., Pardo-Igúzquiza, E., 2014. Millennial- to centennial-scale climate periodicities and forcing mechanisms in the westernmost Mediterranean for the past 20,000 yr. *Quaternary Research* 81, 78-93.

Rull, V., González-Sampériz, P., Valero-Garcés, B., Corella, P., Morellón, M., 2011.

Vegetation changes in the southern Pyrenean flank during the last millennium in relation to climate and human activities: the Montcortès lacustrine record. *Journal of Paleolimnology* 46 (3), 387-404.

Schulte, L., 2002. Climatic and human influence on river systems and glacier fluctuations in southeast Spain since the Last Glacial Maximum. *Quaternary International* 93–94, 85–100.

Schultz, M., Mudelsee, M., 2002. REDFIT: estimating red-noise spectra directly from unevenly spaced paleoclimatic time series. *Computers and Geosciences* 28, 421–426.

Snowball, I., Sandgren, P., 2001. Application of mineral magnetic techniques to paleolimnology. In: Last, W.M., Smol, J.P. (Eds.), *Tracking Environmental Changes Using Lake Sediments*, vol. 2. Kluwer Academic Publishers, Dordrecht, pp. 217–237.

Trouet, V., Esper, J., Graham, N.E., Baker, A., Scourse, J.D., Frank, D.C., 2009. Persistent positive North Atlantic oscillation mode dominated the Medieval Climate Anomaly. *Science* 324, 78-79.

Turney, C.S.M., Kershaw, A.P., Clemens, S.C., Branch, N., Moss, P.T., Fifield, L.K., 2004. Millennial and orbital variations of El Niño/ Southern Oscillation and high-latitude climate in the last glacial period. *Nature* 428, 306–310.

Valbuena-Carabaña, M., López de Heredia, U., Fuentes-Utrilla, P., González-Doncel, I., Gil, L., 2010. Historical and recent changes in the Spanish forests: a socioeconomic process. *Review of Palaeobotany and Palynology* 162, 492–506.

Valle, F., 2003. *Mapa de Series de Vegetación de Andalucía*. Editorial Rueda, S.I., Madrid.

Wassenburg J.A., Immenhauser A., Richter D.K., Niedermayr A., Riechelmann S., Fietzke J., Scholz D., Jochum K.P., Fohlmeister J., Schroöder-Ritzrau A., Sabaoui A., Riechelmann D.F.C., Schneider L., Esper J., 2013. Moroccan speleothem and tree ring

records suggest a variable positive state of the North Atlantic Oscillation during the Medieval Warm Period. *Earth and Planetary Science Letters* 375, 291–302.

Whitlock, C., Anderson, R.S., 2003. Fire history reconstructions based on sediment records from lakes and wetlands. In: Veblen, T.T., Baker, W.L., Montenegro, G., Swetnam, T.W. (Eds.), *Fire and Climatic Change in Temperate Ecosystems of the Americas*, vol. 160. Springer-Verlag, New York, pp. 3-31. *Ecological Studies*.

Figure captions

Figure 1. Location of the Borreguil de la Caldera (BdlC) in Sierra Nevada southern Iberian Peninsula, Mediterranean region. Panel on below left is the general location of BdlC, showing the major peaks in the mountain range, and other previously studied wetlands: BdlV = Borreguil de la Virgen peat bog (Jiménez-Moreno and Anderson 2012); LdRS = Laguna de Rio Seco (Anderson et al., 2011); LdlM = Laguna de la Mula (Jiménez-Moreno et al., 2013b). Panel on below right shows the location of BdlC respect to the upper elevation Laguna de la Caldera and the location of the BdlC-01 where the core was taken.

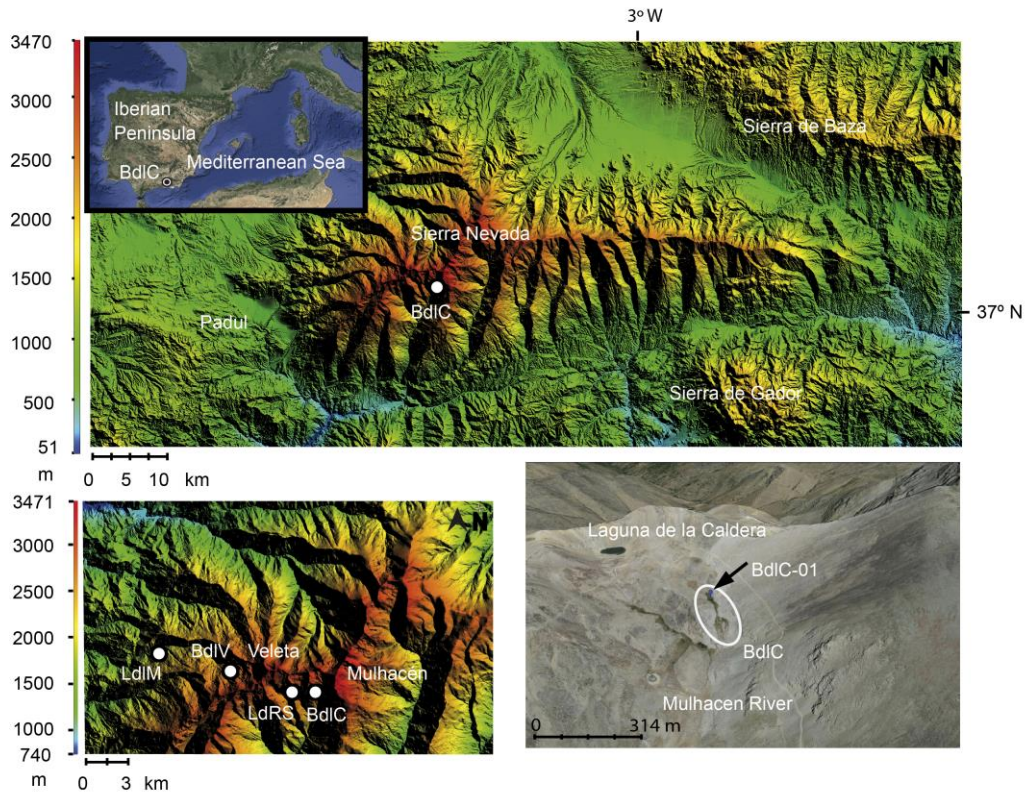


Figure 2. Photo of core BdlC-01, along with the magnetic susceptibility (MS) profile and age-depth model. Sedimentary rates (SAR) are marked. Thin black lines show the 95% confidence intervals. See body of text for explanation of age model construction.

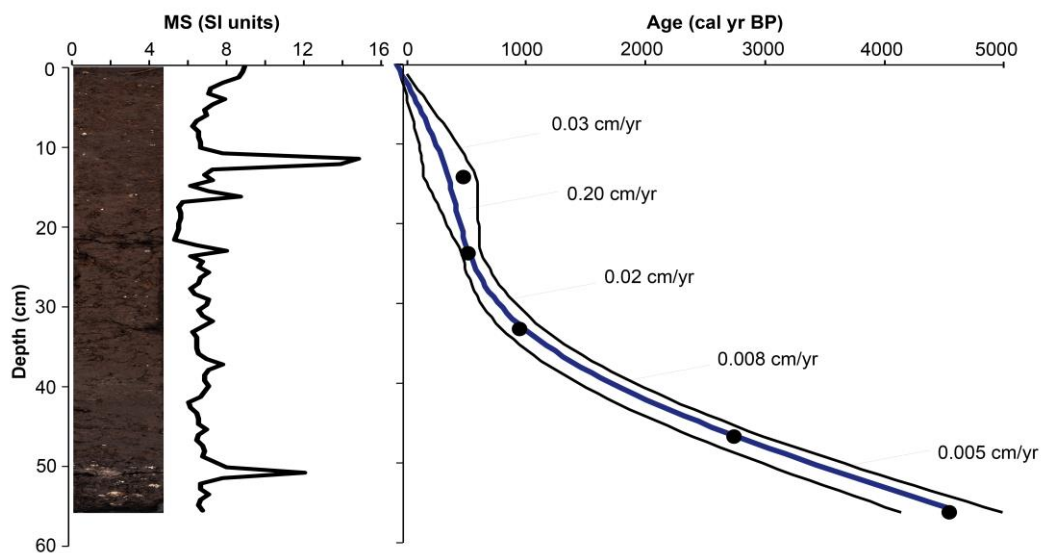


Figure 3. Pollen and non-pollen palynomorphs (NPPs) percentage of selected taxa and charcoal concentration in the BdlC-01 core. Pollen percentage was calculated with

respect to the total pollen sum, excluding Cyperaceae. NPP percentages were calculated with respect to the total pollen sum. Tree taxa are shown in green, herbs and grasses in yellow, aquatic plant in blue and NPPs in orange. Charcoal concentration (number of particles/cc = #/cc), pollen concentration (grains/cc) and pollen zonation are shown on the right. Silhouette shows exaggeration of pollen percentage X5.

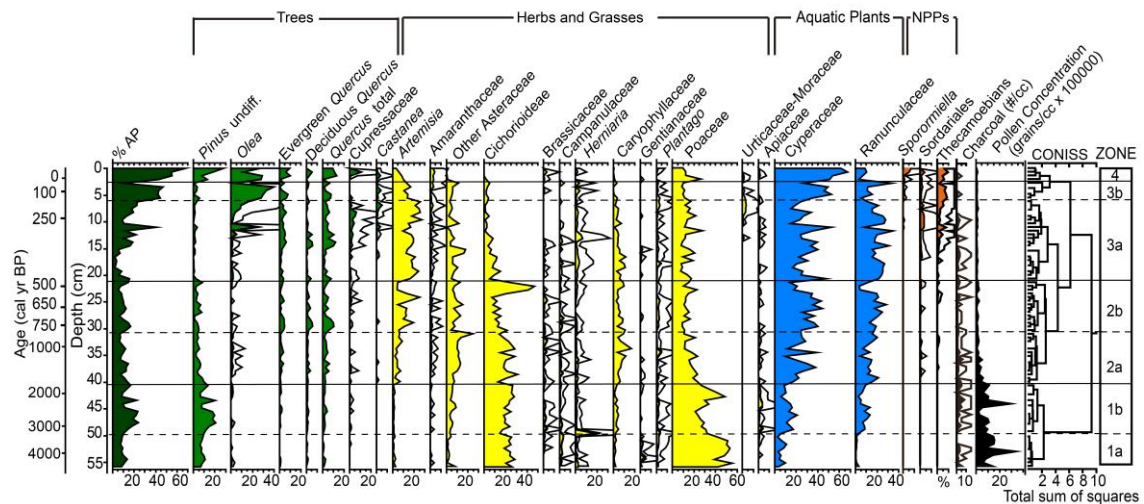


Figure 4. Comparison of different pollen taxa from the last 4500 yr from the BdIC and other pollen records from other Sierra Nevada lakes and peat bogs, North Atlantic Oscillation (NAO) reconstructions and insolation curve. (a) NAO index from a climate proxy reconstruction from Morocco and Scotland (Trouet et al., 2009). (b) NAO index from a climate proxy reconstruction from Greenland (Olsen et al., 2012). (c) BdIC charcoal record. (d) BdIC Magnetic Susceptibility (MS) record. (e) Cyperaceae/Poaceae (C/P) ratio from the BdIC record. (f) *Artemisia* percentage from the BdIC record. (g) *Pinus* percentage from the BdIC record. (h) Arboreal pollen (AP) percentage from the BdIC record. (i) AP percentage from LdlM record (Jiménez-Moreno et al., 2013), Sierra Nevada. (j) *Pinus* percentage from BdIV record (Jiménez-Moreno and Anderson, 2012), Sierra Nevada. (k) *Pinus* percentage from LdRS (Anderson et al., 2011), Sierra Nevada. (l) Winter [left] and summer [right] insolation calculated for 37° N (Laskar et al., 2004).

IRHP = Iberian-Roman Humid Period, DA = Dark Ages, MCA = Medieval Climatic Anomaly. Dashed black lines show a tentative correlation between the *Pinus* record (g) and the NAO reconstruction (b). Color vertical bars highlight discussed climate variability. The green bar represents a relative humid period, the yellow bar an arid period, the blue bar a humid period corresponding with the IRHP and the gray bar a generally arid period.

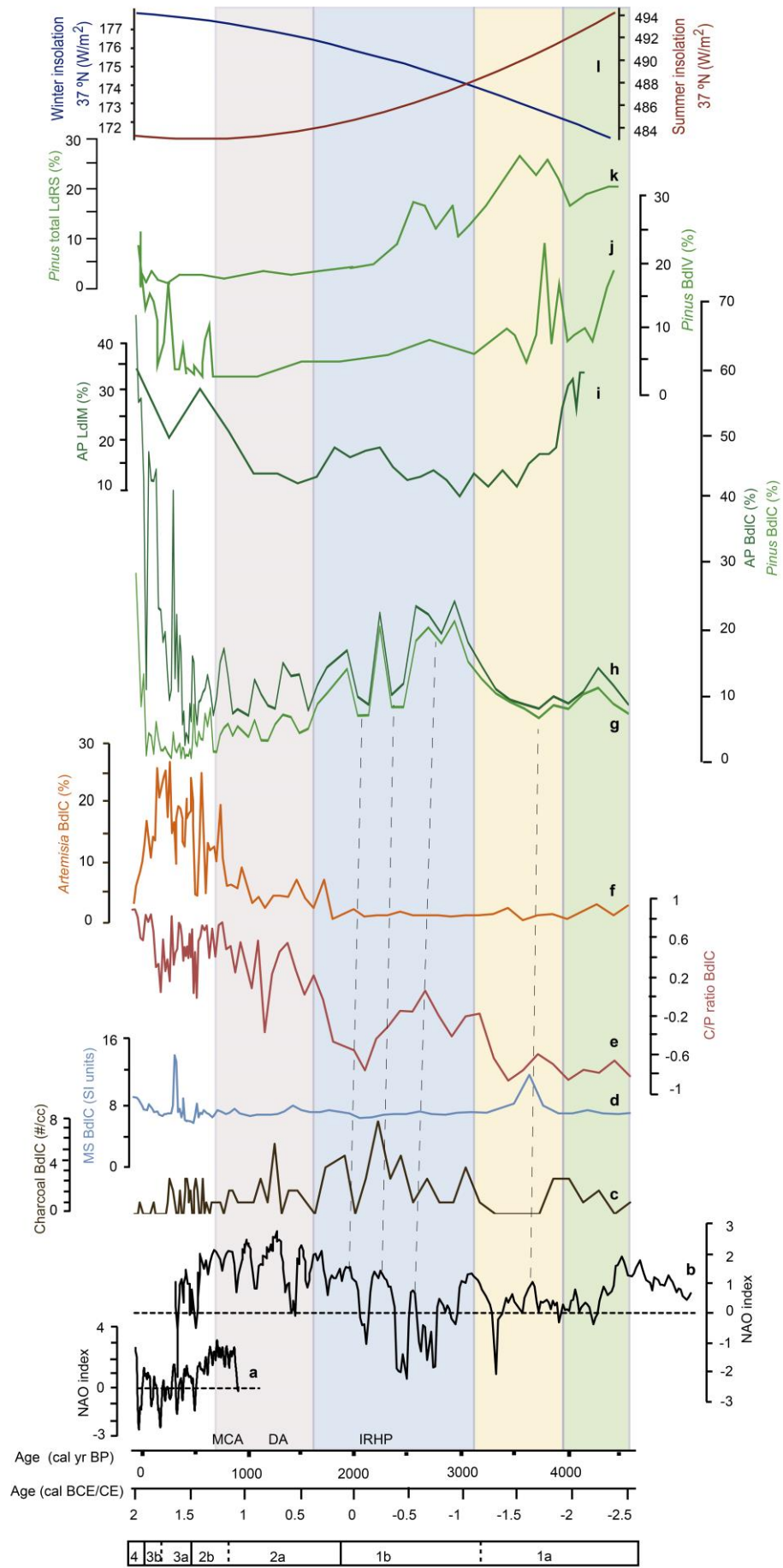


Figure 5. Spectral analysis of *Pinus* and *Artemisia* from the BdlC-01 record. Confidence levels (CI) are marked (80 and 90 %) and the significant periodicities above 80% of confident level are shown. A number of overlapping (50%) segments (n_{seg}) of 3 and a rectangular window were used. Spectral analysis was made using Past (http://palaeo-electronica.org/2001_1/past/issue1_01.htm).

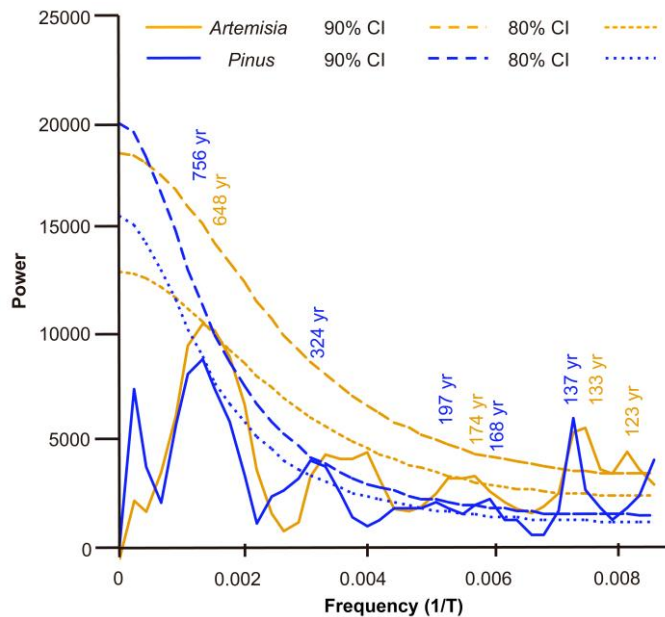


Figure 6. Comparison of different pollen taxa from the last 700 yr from the BdlC record, NAO reconstruction and solar irradiance curve. (a) *Artemisia* percentage from the BdlC record. (b) *Pinus* percentage from the BdlC record. (c) Arboreal pollen (AP) percentage from the BdlC record. (d) North Atlantic Oscillation (NAO) index from a climate proxy reconstruction from Morocco and Scotland (Trouet et al., 2009). (e) North Atlantic Oscillation (NAO) index from a climate proxy reconstruction from Greenland (Olsen et al., 2012). (f) Reconstruction of the total solar irradiance (Bard et al., 2000). Dashed black lines are a tentative correlation between *Artemisia* record (a) and NAO reconstruction (d, e). Dashed red lines show a tentative correlation between the *Pinus* record (b) and solar activity (f).

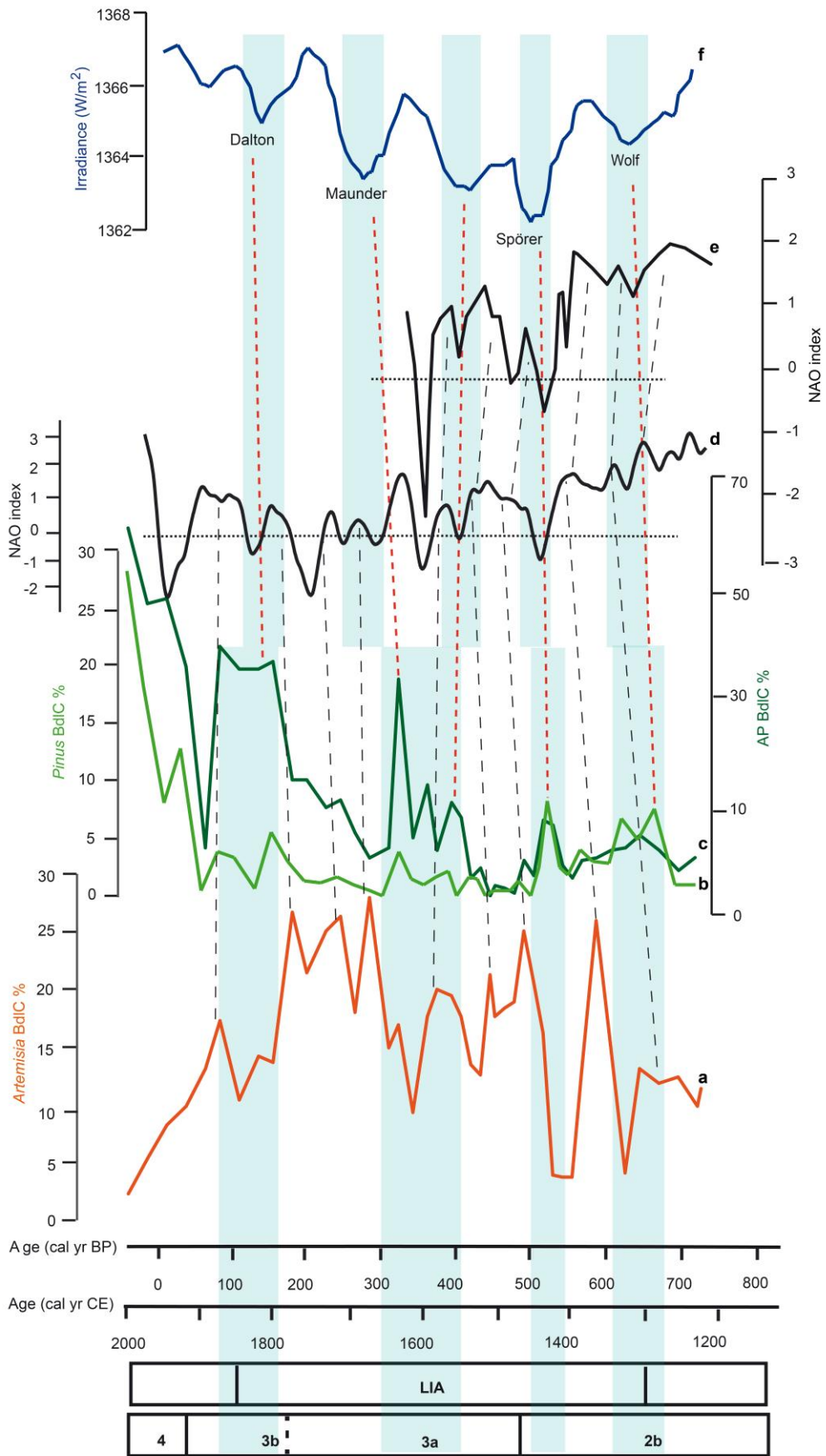


Figure 7. Comparison of pollen and non-pollen palynomorphs (NPPs) for the last 4500 cal yr BP from the BdlC-01 core considered to be related to human activities. Note the exponential increase in the taxa in the last 400 cal yr BP: *Olea* pollen, Sordariales, *Sporormiella* and thecamoebians. The gray vertical bar represents evidences of human impact in the last 400 cal yr BP.

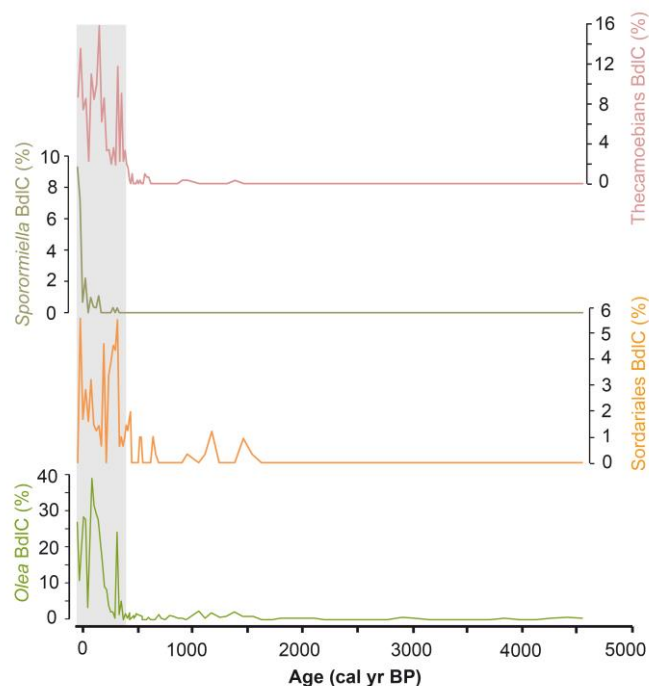


Table 1. Age data for BdlC-01. All ages were calibrated using IntCal13 curve (Reimer et al., 2013) with Calib 7.1 (<http://calib.qub.ac.uk/calib/>).

| Laboratory number ^a | Depth (cm) | Dating method (AMS) | Age (14C cal yr BP \pm 1 σ) | Calibrated age (cal yr BP) 2 σ range | Median age (cal yr BP) |
|--------------------------------|------------|---------------------|---------------------------------------|---|------------------------|
| Reference ages | 0 | Present | AD2013 | -63 | -63 |
| DirectAMS-004385 | 13.7 | ¹⁴ C | 388+24 | 327-507 | 469 |
| DirectAMS-004386 | 23.2 | ¹⁴ C | 474+26 | 500-537 | 517 |
| DirectAMS-004387 | 36.8 | ¹⁴ C | 1036+31 | 915-1049 | 950 |
| DirectAMS-004388 | 46.4 | ¹⁴ C | 2563+30 | 2505-2754 | 2725 |
| DirectAMS-004389 | 56 | ¹⁴ C | 4066+29 | 4438-4798 | 4551 |

*Sample number assigned at radiocarbon laboratory; DirectAMS= Accium BioSciences, Seattle, Washington.